JOURNAL OF GEOPHYSICAL RESEARCH, VOL. 101, NO. C6, PAGES 14,095–14,109, JUNE 15, 1996

Energy-containing scales of turbulence in the ocean thermocline

J. N. Moum

College of Oceanic and Atmospheric Sciences, Oregon State University, Corvallis

Abstract. From measurements of the energy-containing scales of turbulence in the ocean thermocline, two new formulations are examined: (1) an inviscid estimate for the viscous dissipation rate of turbulent kinetic energy and (2) a mixing length estimate for the turbulent heat flux. These formulations are tested using coincident measurements of the relevant properties of both energy-containing and dissipation scales of stratified turbulence in the ocean's main thermocline obtained from a vertical microstructure profiler. It is found that energy-containing scale estimates of both dissipation rate and heat flux compare favorably with dissipation scale estimates. Since the energy-containing scales are many times greater than the dissipation scales, the measurement constraints on these new estimates are considerably less strict than for dissipation scale estimates of the same quantities. These observations also suggest that the timescale for viscous decay of turbulent motions is greater than that for diffusive smoothing of scalar fluctuations. It is argued that this is consistent with current estimates of mixing efficiencies.

1. Introduction

To understand quantitatively or even qualitatively, the role of turbulence in the ocean, we must obtain both more comprehensive data coverage in space and time and the capability to measure more turbulence variables. Most of our oceanic observations of turbulence have been made from vertical profilers. Although well resolved in the vertical, the data samples represent vertical lines through turbulent flow fields of unknown spatial extent at some unknown point in their temporal evolution. While they provide a different perspective, similar limitations hold for horizontal measurements. It is important that we find new ways to improve our space-time resolution of turbulent flow fields in the ocean.

To date, virtually all oceanic turbulence measurements have been of either (sometimes both) the smallest scales of the temperature or of the velocity gradient fluctuations. From these measurements, the dissipation rates of temperature variance and turbulent kinetic energy (TKE) are computed. However much we have learned from these measurements, they are only partial representations of the turbulence, and conclusions based on them depend heavily on inference.

Studies of atmospheric turbulence have benefited from a more varied array of sensors and platforms [e.g., *Lenschow,* 1986]. These include means of measuring the size, velocities, and temperature perturbations associated with the energy-containing scales of the turbulence. Since the energy-containing scales of these fields are considerably larger than the dissipation scales, they can generally be measured more easily and using remote sensing techniques, more rapidly. A key component of these measurements is the vertical velocity component of the turbulence. From this measurement, the vertical transports of heat, momentum, and other constituents can be assessed. As well, it provides a measure of the TKE itself. Now that we have learned how to measure this component in the ocean [*Moum,* 1990a,b], we can begin to consider new methods of investigating turbulent fields, based on measurements of the energy-containing eddies.

The physical dimension of motion in turbulent flows is limited at the smallest scales by viscous forces. This dimension is determined by the Kolmogoroff scale, $\eta = (\nu^3/\epsilon)^{1/4} = k_s^{-1}$, where ν is the kinematic viscosity and ϵ is the viscous rate of dissipation of TKE. This length scale is that at which inertial forces equal viscous forces. In the ocean, η can be as small as $O(10^{-3}$ m) in the most intense turbulence. The spectrum of ϵ peaks at about (0.1-0.2)k_s [*Gargett et al.,* 1984; *Moum,* 1990a]. The equivalent Kolmogoroff velocity scale, $u_s = (\nu\epsilon)^{1/4}$, may be as small as $O(10^{-4}$ m s^{-1}). This means that the measurement required to compute ϵ directly (from $\epsilon \simeq (15/2)\nu\overline{(\partial u/\partial z)^2}$ must resolve 10^{-4} m s^{-1} velocity fluctuations over 10^{-3} m spatial separations and should, in principle, include all components of $\epsilon = \nu\overline{(\partial u_i/\partial x_j)[(\partial u_i/\partial x_j) + (\partial u_j/\partial x_i)]}$. In practice, although we frequently refer to direct measurement of ϵ, this degree of resolution is not achieved

Paper number 96JC00507.
0148-0227/96/96JC-00507$09.00

with present sensors deployed in the ocean, and consequently, spectral corrections are required [*Moum et al.*, 1995]. Since, at most, 2 (of 12) terms in the dissipation tensor are measured, we generally assume the turbulence is isotropic to estimate ϵ, thereby introducing another source of uncertainty.

The energy-containing scales of the turbulence represent the large eddies of the turbulence and are dictated by different physics from those affecting the dissipation scales. For example, in a boundary layer, the size of the energy-containing eddies is limited by the boundary layer's thickness and by proximity to the boundary as the boundary is approached. For reference, let ℓ represent the length scale and u the velocity scale typical of the energy-containing eddies. In general, the energy-containing scales of the turbulence in the ocean's thermocline are at least an order of magnitude greater in both physical dimension and amplitude of velocity fluctuations than the dissipation scales. Hence they are easier to detect, and it is of practical importance that an evaluation be made of these scale relations.

Length Scales

Several specific length scales, which can be determined observationally, prove useful in defining the role of the energy-containing eddies as follows: The Thorpe scale L_t is computed by sorting a highly resolved density profile into its monotonic equivalent [*Thorpe*, 1977]. It is generally considered as an rms quantity; unless otherwise noted, L_t is intended to represent the rms value over the record; in this study, a record consists of a single turbulent patch (discussed below). L_t represents a kinematic (as opposed to a dynamic) definition. For the purpose of this analysis, the buoyancy frequency, $N^2 = -g\rho_o^{-1}\rho_z$, was determined from the Thorpe-reordered density profile and is intended to represent the background stratification against which the turbulence must work.

In a stratified fluid away from boundaries, the size of the largest eddies is limited by the work required to counter buoyancy forces. The length scale at which buoyancy forces equal inertial forces is the Ozmidov scale $L_o \equiv (\epsilon/N^3)^{1/2}$ (following the scaling of *Gargett* [1988]). *Gargett et al.* [1984] demonstrated the departure from local isotropy at length scales greater than L_o using stratified turbulence data obtained in a tidal flow over an estuarine sill. Presumably, this represents the effects of the stratification on the energy-containing scales. In the main thermocline ($N \approx 0.005$ s^{-1}), typical values of ϵ give $L_o \approx 1$ m or less. From measurements in the wind-mixed layer of a lake and the seasonal thermocline of the ocean, *Dillon* [1982] demonstrated that L_t and L_o were highly correlated and $L_t \approx 1.2L_o$.

The buoyancy length scale, $L_b \equiv w/N$, represents the vertical distance traveled by a particle if all of its vertical kinetic energy is converted to potential energy (i.e., if $N^2L_b^2 = w^2$). Here L_b and w represent rms length and velocity scales, respectively. Since the conversion of kinetic to potential energy is less than 100% efficient, L_b is the largest vertical scale of the energy-containing eddies. From laboratory measurements, *Lienhard and Van Atta* [1990] demonstrated L_b to be an upper bound on L_t.

Another length scale is akin to that proposed by *Ellison* [1957]. $L_e = [\overline{\rho'^2}]^{1/2}/\overline{\rho}_z$ represents a typical vertical distance a fluid particle travels before either returning to its equilibrium level or mixing. Here ρ' is the fluctuating density and $\overline{\rho}_z$ is the vertical gradient of the mean density. If density is determined primarily by temperature, then we can substitute temperature for density and $L_e = [\overline{T'^2}]^{1/2}/\overline{T}_z$. The fluctuation temperature used for the present analysis is the deviation of the in situ profile from the Thorpe-reordered profile (as prescribed by *Moum* [1996]). Estimates of L_e from horizontal profiles will include the influence of internal gravity waves. Estimates from vertical profiles, determined in this way from reordered temperature profiles, limit the influence of nonturbulent motions. Laboratory results in which L_e was estimated from horizontal profiles but internal waves were presumed to have minimal influence indicated $L_e \approx L_t$ [*Itsweire*, 1984]. Numerical simulations for which the density fluctuation was defined relative to a volume average indicated $L_e \approx 0.8L_t$ [*Itsweire et al.*, 1993].

Inviscid Estimate of ϵ

An inviscid estimate of ϵ was proposed by *Taylor* [1935], based solely on dimensional reasoning. A more physical argument is based on the notion that a considerable fraction of the TKE $\sim$ u^2 is dissipated in the time $\tau = \ell/u$ required for an eddy of size ℓ with typical velocity u to turn over. That is, the rate at which TKE is lost to viscous dissipation is proportional to $u^2/\tau \sim u^2/(\ell/u) = u^3/\ell$. This argument is presented by *Frisch and Orszag* [1990], among others. As *Gargett* [1994] points out, although this concept was introduced for unstratified fluids, it is expected to hold even in stratified fluids as the energy lost to increasing the potential energy by working against buoyancy forces is thought to be a small fraction of the TKE. This relation can be written as

$$\epsilon = C_\epsilon \frac{u^3}{\ell}, \tag{1}$$

where C_ϵ is a constant of proportionality to be determined empirically. This estimate employs neither the scales directly affected by ν nor ν itself. It is based on the energy-containing scales of the turbulence and is independent (observationally) of the viscous estimate, which requires resolution of the dissipation scales of the turbulence [*Moum et al.*, 1995].

Fluxes

The most significant aspect of three-dimensional turbulence in stratified fluids is its capacity to enhance the irreversible transfer of mass and momentum. However, we only have a rudimentary understanding of the rate at which mixing occurs in the ocean thermocline and where and when to expect the intermittent instances of energetic turbulence which appear in our observations as distinctive patches in the stratified fluid. In large part, this is because very little relevant data have been obtained in proportion to the great scale and time variability of the ocean; but also, there is considerable concern about the validity of indirect estimates of turbulent fluxes of heat and density determined from microstructure measurements. These methods are based on measurements of the dissipation rates of TKE, ϵ, and temperature variance χ.

From a steady state balance of the TKE equation, *Osborn* [1980] derived what is sometimes termed the dissipation method, in which the turbulent heat flux F, as it is represented by the correlation of vertical velocity and temperature fluctuation in the evolution equation for TKE, is approximated by

$$F \equiv \langle w'T' \rangle \simeq \Gamma_o \epsilon \frac{T_z}{N^2} \equiv \Gamma_o F_\epsilon, \qquad (2)$$

where T_z is the vertical gradient of mean temperature, $\Gamma_o = R_f/(1-R_f)$, and R_f is the flux Richardson number. The notation follows that used by *Gargett and Moum* [1995] and *Moum* [1996]. The representation of F by $\Gamma_o F_\epsilon$ requires a TKE balance between shear production s, buoyancy flux b, and ϵ. In a stably stratified fluid, the buoyancy flux always represents a loss of TKE which is in addition to dissipative losses. The shear production is the only source term. Strictly speaking, $R_f = b/s$ is a mixing efficiency since it represents the ratio of the rate of increase of the system's potential energy to the rate at which TKE is produced. The parameter $\Gamma_o = b/\epsilon$ is not a mixing efficiency, although we in the community have referred to it as such. It is simply related to R_f, however, and comparison of results which evaluate R_f and those evaluating Γ_o is straightforward. *Moum* [1996] and *Gargett and Moum* [1995] advocate using the term dissipation flux coefficient for Γ_o to avoid future confusion.

An alternative method [*Osborn and Cox,* 1972], derived from a steady state balance for fluctuation temperature (originally entropy), gives

$$F \simeq 0.5\chi/T_z \equiv F_\chi. \qquad (3)$$

Coincident measurements of F_ϵ and F_χ yield the following estimate of Γ_o:

$$\Gamma_d = F_\chi/F_\epsilon. \qquad (4)$$

Oceanic observations indicate mean values of $\Gamma_d \approx 0.1$-0.4 (summarized by *Moum* [1990a]). Flux measurements in laboratory flows imply $\Gamma_o \approx 0.2$ [*Rohr and Van Atta,* 1987]. Eddy-correlation measurements in oceanic regimes indicate values of Γ_o ranging from 0.05 [*Yamazaki and Osborn,* 1993; *Fleury and Lueck,* 1994] to 0.15–0.2 [*Moum,* 1996], while the tidal front measurements of *Gargett and Moum* [1995] indicate $\Gamma_o \simeq 0.7$.

Another heat flux estimate is based on the concept of a mixing length (attributed to Prandtl, *Tennekes and Lumley* [1972]). If the turbulent motions are considered analogous to molecular motions, then a turbulent eddy viscosity K_v can be defined as the product of a representative velocity fluctuation and length scale. In a flow field in which turbulent Prandtl number, $Pr = K_v/K_h = 1$, this may also be extended to define an eddy diffusivity K_h. Consequently, we have another flux estimate,

$$F_\ell \equiv C_\ell u \ell T_z, \qquad (5)$$

where C_ℓ is a constant of proportionality. Measurements in the atmospheric boundary layer indicated $C_\ell \approx 0.2$, where the rms vertical velocity was substituted for u and L_b for ℓ [*Hunt et al.,* 1985]. This formulation has not previously been tested from measurements in any oceanic regime that I know of.

While the eddy-correlation flux, $\langle w'T' \rangle$, was evaluated from the data set considered here, the issues of how to compute $\langle w'T' \rangle$, how to assess uncertainties, and how to interpret the results, are not straightforward. These issues are addressed in another paper [*Moum,* 1996]. Instead, this paper focuses on the deductions that can be made from the energy-containing scales of the turbulence.

The purposes of this paper are as follows: (1) to establish the relationships between observationally derived length scales in well-defined turbulent patches in the main thermocline of the North Pacific Ocean (an unspecified length scale appears in both (1) and (5); hence, before (1) and (5) can be usefully evaluated, the appropriateness of the proposed length scales that can be estimated from the data must be determined); (2) to compare viscous and inviscid estimates of ϵ and to provide a convenient formulation for (1); (3) to compare energy-containing scale heat flux estimates to dissipation heat flux estimates, with the intent of providing a convenient formulation for (5); and (4) to evaluate the decay rates of both temperature variance and TKE in turbulent patches.

2. Experimental Details

It is a characteristic of vertical records of turbulent patches in the ocean's thermocline that very few and short stretches of the records exhibit turbulence, which is sufficiently energetic to be detected by existing measurement systems [e.g., *Gregg,* 1987]. For the purpose of comparing turbulence quantities, it is unreasonable to include data with no detectable signal together with data representing the energetic parts of the record. Consequently, this analysis focuses on the energetic parts of the records or the clearly turbulent patches within the thermocline. A rationale for data selection follows.

To be considered for this analysis, the data were required to meet several conditions. These constitute the definition of turbulent patch used here: (1) to avoid ambiguities in the designation of temperature fluctuation as the difference between in situ and reordered temperature, only data for which the stratification was determined principally by temperature were used; (2) to avoid inclusion of noise with signal, only data with all fluctuation signals significantly different from their respective noise levels were used; (3) only turbulent patches with well-defined upper and lower boundaries between turbulent fluid and ambient fluid were selected for analysis (the specific requirement is that $\int L_t(z)dz = 0$ between these boundaries; this is discussed in more detail by *Moum* [1996], who provides examples that help in visualising this condition); and (4) only turbulent patches in which the energy-containing scale ℓ was less than 3 m were selected.

This fourth condition serves to minimize the attenuation of the vertical velocity spectrum at the energy-containing scales. As the profiler body is 4.2 m long (as in the work by *Moum et al.* [1995]) and falls freely, it will act as a high-pass filter to scales $\approx$ 4 m and larger. In flow regimes with very large energy-containing scales such as turbulent tidal fronts [*Gargett and Moum,* 1995], it is most likely that w is poorly resolved by this type of measurement. A more reasonable flow regime for evaluation, especially for these initial comparisons, is the main thermocline where the combination of moderate to strong stratification and low to moderate turbulence levels should result in sufficiently small length scales.

A consequence of the high-pass filtering of w is that the mean value of w is nearly zero for a particular patch. To further ensure the complete removal of inadequately resolved low-frequency motion, a symmetric high-pass filter of length equivalent to 3.75 m was run over the w data. A fixed scale separation is introduced by this procedure. It is possible that, in some cases, some vertical motion at scales >3.75 m has been excluded from the analysis that we should properly consider to be part of the turbulence. It is also possible that we have included some vertical motion at scales <3.75 m that should be considered part of the internal gravity wave field or, more likely, part of the ill-defined range of scales bounded by waves and fully developed turbulence. The rationale for the selection of patches was intended to minimize this crosstalk of scales.

The data selected for this analysis were obtained in the spring of 1991, approximately 1000 km off the coast of northern California (39°N, 135°15'W). Over a 6-day period (May 1 to May 7), more than 400 vertical profiles to at least 650 m depth were made using the vertical microstructure profiler Chameleon [*Moum et al.,* 1995]. Prior to and during these measurements, a series of storms excited considerable near-inertial wave activity. Shear layers produced by downward propagating, near-inertial waves were localized at stratified regions of the seasonal thermocline and were sites of intense turbulence. The decay of near-inertial wave energy due to turbulence is the focus of the analysis by *Hebert and Moum* [1994]. In the upper part of the main thermocline, below the region analyzed by Hebert and Moum, turbulent patches were generally thinner and more intermittent (i.e., less frequent). The data considered here all come from the upper part of the main thermocline. A total of 272 turbulent patches from this region met the criteria for analysis, each representing a data point in the analysis to follow.

The energization of the water column by the near-inertial wave may have influenced the turbulence at these depths and provided a greater dynamic range for turbulence parameters than during normal background conditions. However, without a background reference, we cannot know this.

Measurements made from Chameleon included pressure (depth), temperature, conductivity, temperature gradient fluctuations using an FPO7 microbead thermistor, horizontal velocity gradient fluctuations (using airfoil or shear probes), and vertical velocity fluctuations using a pitot tube [*Moum,* 1990b]. Salinity and density were determined from temperature and conductivity. The temperature variance dissipation rate χ was determined from temperature gradient fluctuations. Because the thermistor does not fully resolve the spectrum of temperature gradient variance, a correction was applied, based on the Batchelor form of the scalar variance spectrum (the correction is given by *Peters et al.* [1988]). The TKE dissipation rate ϵ was determined from horizontal velocity gradient fluctuations. Details of the computation are discussed by *Moum et al.* [1995]. An examination of some individual examples of the turbulent patches analyzed here is provided by *Moum* [1996].

3. Results

Turbulent Length Scales

The patches selected for analysis, based on the requirements listed in section 2, range in thickness from 0.5 to 15 m (the patch thickness L_p is the vertical distance between upper and lower boundaries of the patch). This is roughly (3–75)$\times L_t$ and follows no particular pattern (Figure 1a). L_p is always greater than the maximum value of L_t in the patch ($L_t^{\max}$), as required by the selection criteria (Figure 1b). There is a strong correspondence between L_t and $L_t^{\max}$, indicating $L_t^{\max} \approx 3.3 L_t$ (the constant of proportionality used

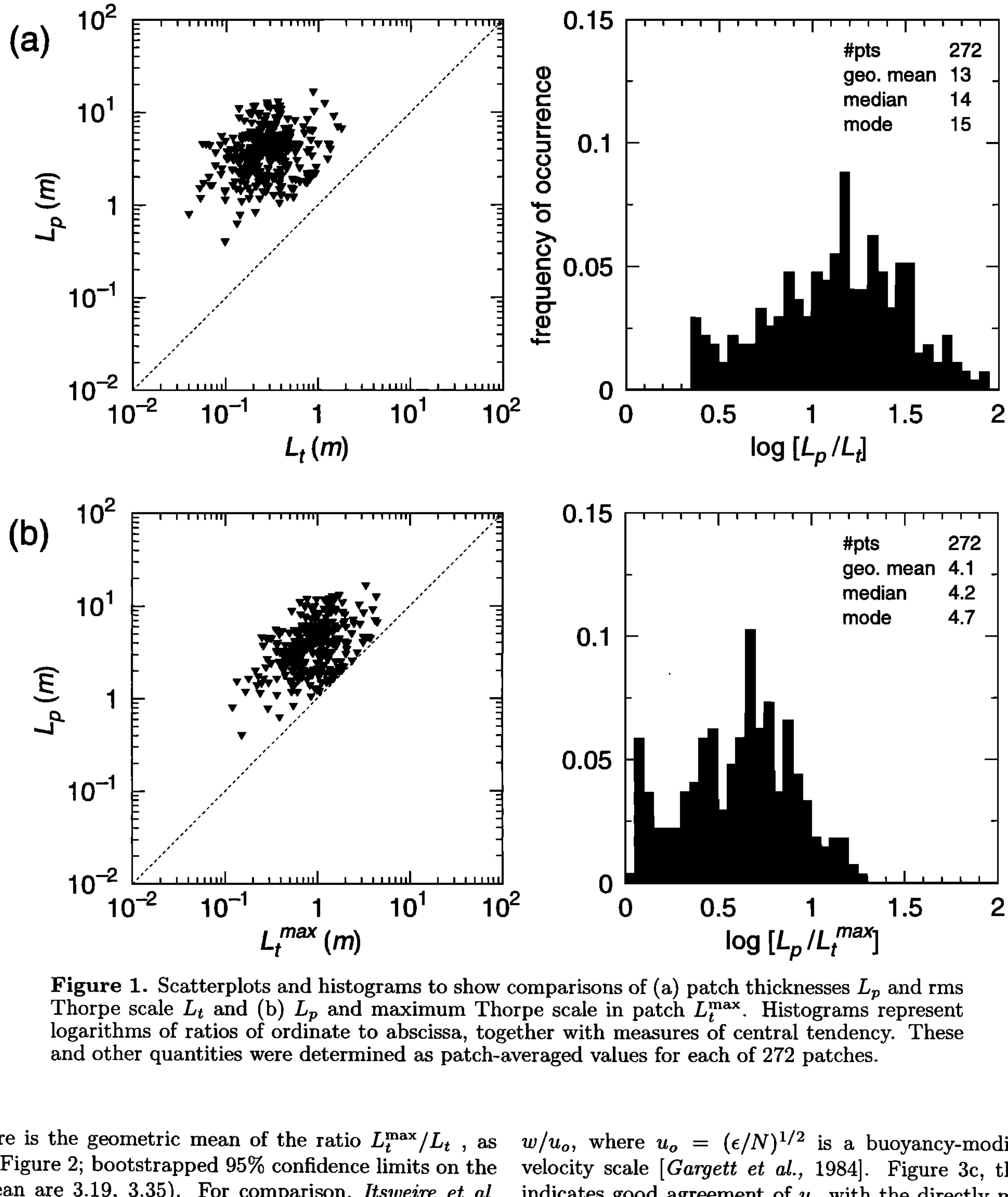

Figure 1. Scatterplots and histograms to show comparisons of (a) patch thicknesses L_p and rms Thorpe scale L_t and (b) L_p and maximum Thorpe scale in patch $L_t^{\max}$. Histograms represent logarithms of ratios of ordinate to abscissa, together with measures of central tendency. These and other quantities were determined as patch-averaged values for each of 272 patches.

here is the geometric mean of the ratio $L_t^{\max}/L_t$, as in Figure 2; bootstrapped 95% confidence limits on the mean are 3.19, 3.35). For comparison, *Itsweire et al.* [1986] found $L_t^{\max} \approx 2.74L_t$.

Comparison of the independent length scales L_t, L_b, and L_o indicates $L_t \approx 1.1\ L_o$ (95% confidence limits 1.08, 1.20) and $L_t \approx 1.0\ L_b$ (95% confidence limits 0.97, 1.09; Figure 3). *Dillon* [1982] found $L_t \approx 1.2L_o$, which is not significantly different statistically and should not be expected to be, given the scatter in the data and the sources of uncertainty in estimates of both L_t and L_o. L_e is not independent of L_t. The comparison indicates $L_e \approx 0.6L_t \approx 0.7L_o \approx 0.6L_b$ (Figure 4).

The comparison between L_b and L_o may be interpreted in terms of velocity scales. The ratio $L_b/L_o=$ w/u_o, where $u_o = (\epsilon/N)^{1/2}$ is a buoyancy-modified velocity scale [*Gargett et al.*, 1984]. Figure 3c, then, indicates good agreement of u_o with the directly measured rms velocity scale w (i.e., the rms value of w computed over the patch). This suggests that the energy-containing eddies are indeed inhibited by the stratification and that the vertical velocity scales are well resolved by the measurement.

Inviscid Estimate of ϵ

An assessment of patch rms estimates of w indicates that the smallest values resolved are ≈ 0.4 mm s^{-1} and the largest values are ≈ 5 mm s^{-1} (Figure 5). These roughly follow $\epsilon \propto w^3$. While it is useful to view the data in this form, simply to indicate the range and res-

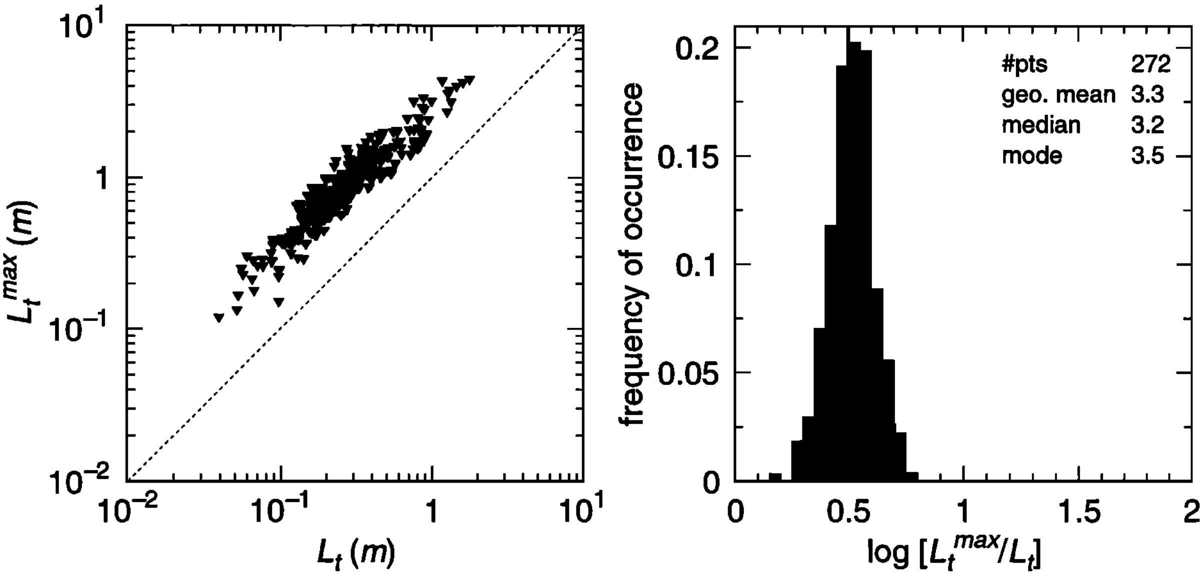

Figure 2. Comparison of L_t and $L_t^{\max}$.

olution of w from these measurements, the correspondence is dimensionally inconsistent. Dimensional correspondence is achieved via the inviscid estimate (1) for ϵ. If the turbulence is isotropic, w^2 is a good estimate of TKE or u^2. From Figure 6, we can see that both the vertical Reynolds number, $Re_w = w\ell/\nu$, and the turbulence activity, $\epsilon/\nu N^2$, are at the lower end of the range of the equatorial data set examined by *Peters et al.* [1995] (whose definition of Reynolds number is based on horizontal not vertical velocity; they refer to it as a turbulent Reynolds number). However, all of the data points are characterized by $Re_w \gg 1$. According to the scalings proposed by *Gargett* [1988], this indicates that the velocity field must be nearly isotropic, i.e., $u \sim w$, and it seems appropriate to use w to represent u in (1).

A demonstration of the approximate equivalence of various observationally derived length scales precedes this discussion. The replacement of ℓ in (1) by these length scales was tested. Replacement of the length scale ℓ with L_e or L_t and the velocity scale u with measured w in the inviscid estimate (1) yields estimates which show considerable scatter in comparison with the viscous estimate (Figures 7b and 7c).

Using either of the length scales L_b or L_o in the inviscid estimate yields the equivalent relation, $\epsilon = C_\epsilon w^3/\ell = aNw^2$ (but with different constants of proportionality; $a = C_\epsilon$ (ℓ=L_b); $a = C_\epsilon^{2/3}$ (ℓ=L_o)). The agreement with the viscous estimate is considerably better (Figure 7a) than it is with either of the kinematic length scales L_e or L_t, indicating $\epsilon \approx 0.73Nw^2$ (95% confidence limits on the coefficient 0.67, 0.79) over 4 orders of magnitude. The constant of proportionality, $a \approx 0.7$ ($C_\epsilon \approx 0.7$, if $\ell = L_b$, or $C_\epsilon \approx 0.6$, if $\ell = L_o$).

Flux Estimates

The comparisons of flux estimates are made in kinematic heat flux units, that is Kelvin meters per second, the result of the product of a diffusivity and mean temperature gradient or the correlation of vertical velocity fluctuation and temperature fluctuation. These comparisons show general agreement between all of the indirect flux estimates F_ϵ, F_χ , including the mixing length estimates (F_{L_b} represents F_ℓ with L_b as the mixing length). This is evident in Figures 8 and 9. The ratio $\Gamma_d = F_\chi/F_\epsilon$ is about 0.25–0.33 (Figure 8a), within the ranges of other estimates (*Moum* [1990a], including that obtained by *Gargett and Moum* [1995] from data obtained in a turbulent tidal front). The agreement between F_{L_b} and F_ϵ is at least as good as that between F_ϵ and F_χ. Using L_e as the mixing length to estimate F_ℓ (represented as F_{L_e}) provides an apparently closer agreement (smaller standard deviation) with F_ϵ and F_χ than F_{L_b} does (Figure 9).

The formulation F_{L_b} reduces to a convenient expression, $F_{L_b} = C_\ell u\ell T_z = C_\ell(w^2/N)T_z$, where $C_\ell \approx 0.24$ (95% confidence limits 0.21, 0.27). This requires estimates of only the background stratification, temperature gradient, and the energy-containing velocity scale. The other forms for F_ℓ require more finely resolved measurements to determine the length scales.

Decay Timescales of the Energy-Containing Eddies

An assessment of the lifetimes of the energy-containing scales of stratified turbulence was first made from observations by *Dillon* [1982]. T' was defined (as here)

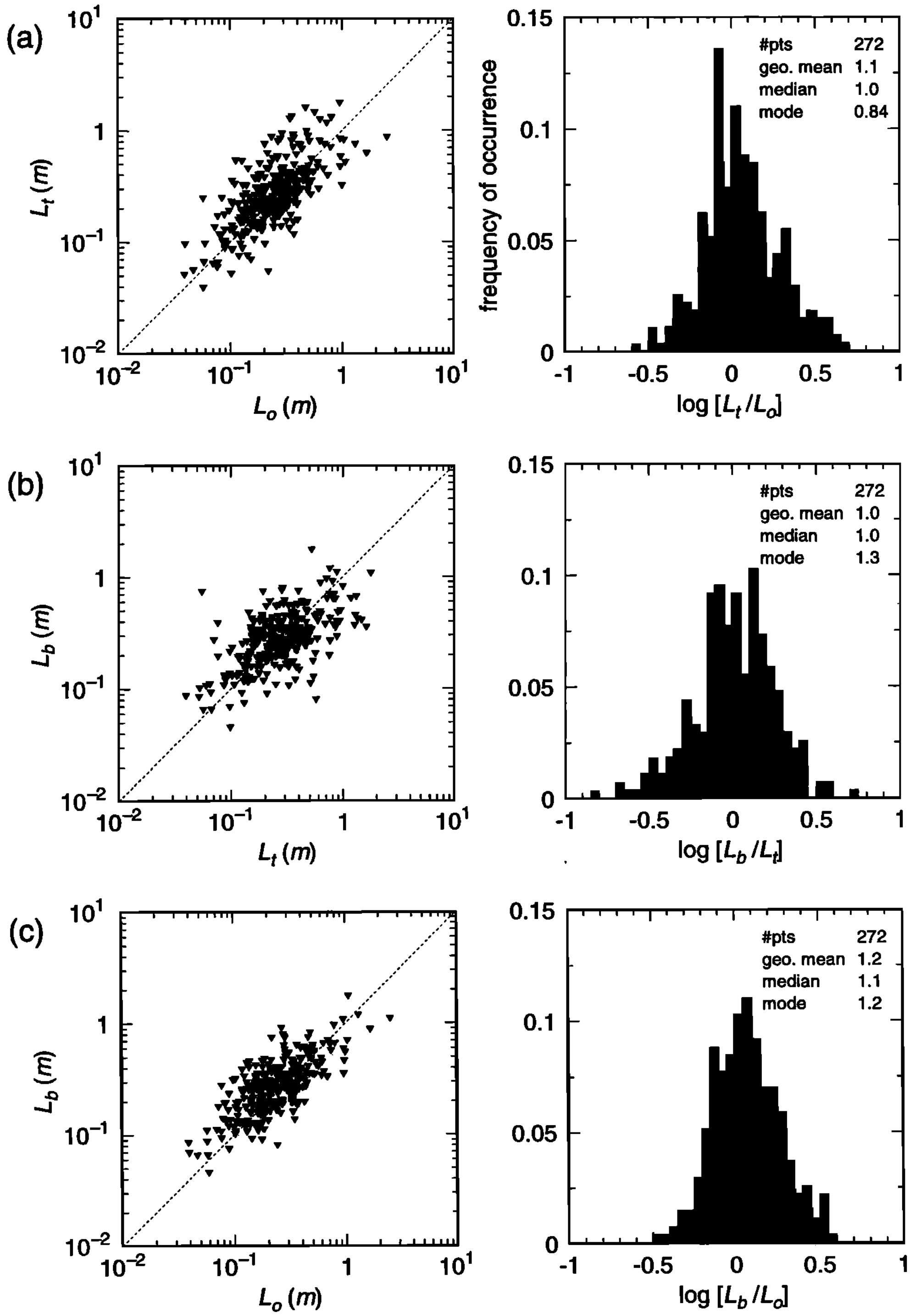

Figure 3. Comparisons of length scales (a) L_t versus Ozmidov scale L_o, (b) buoyancy length scale L_b versus L_t, and (c) L_b versus L_o.

to be the difference between in situ and reordered temperature profiles, where the reordered temperature (or density) profile represents the lowest possible potential energy state of the observed temperature distribution. This lowest potential energy state can only be achieved, in the absence of continued production of temperature variance ($\overline{T'^2}$), by full gravitational collapse of the fluid in the patch, with no diffusive smoothing. That is, it can only be achieved if it occurs on a timescale that is short compared to the time required for diffusive smoothing. The diffusive timescale is given by

$$\tau_T = \frac{\overline{T'^2}}{\chi} \quad (6)$$

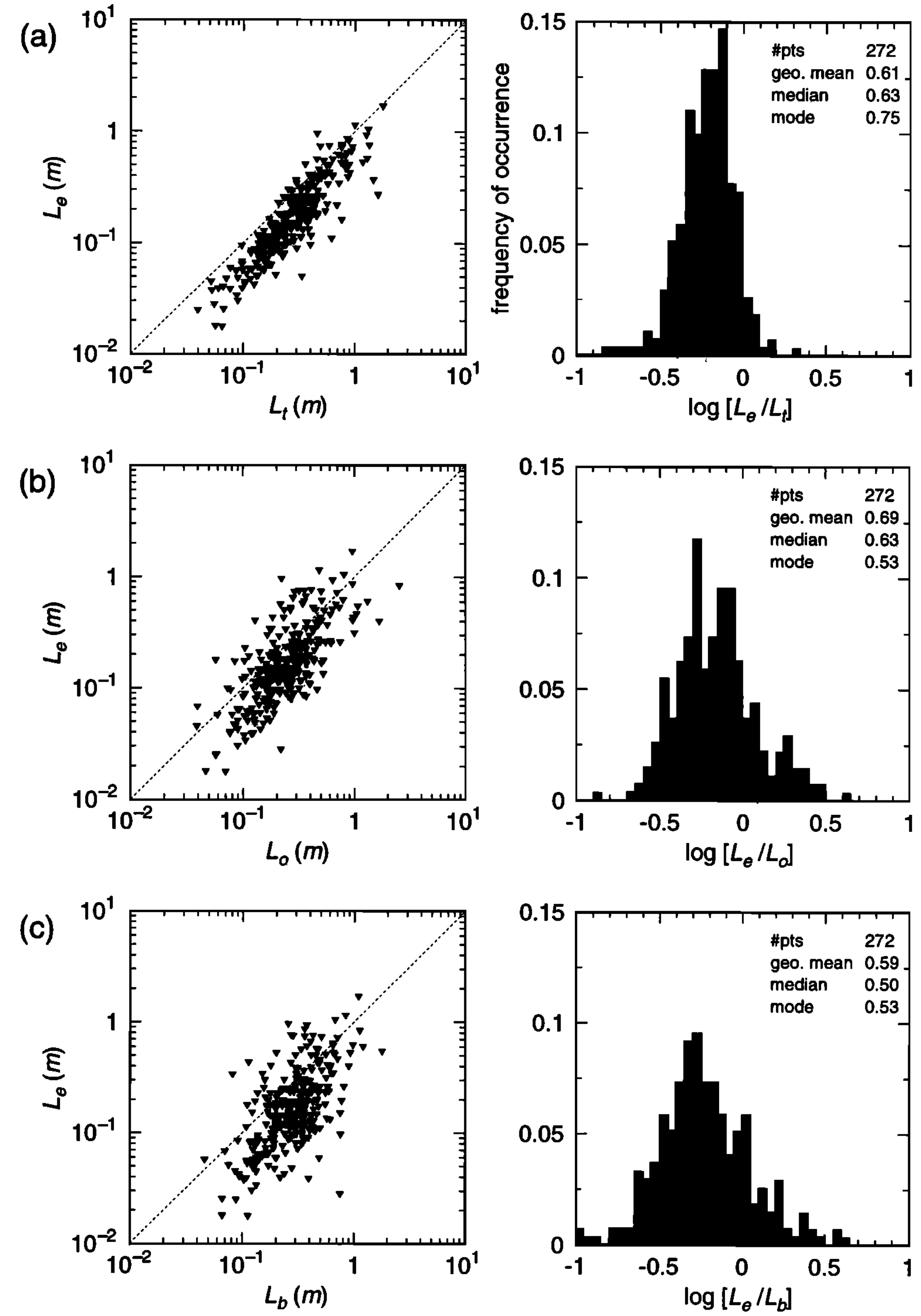

Figure 4. Comparisons of length scale which represents a typical distance a particle travels before returning to equilibrium or mixing L_e with (a) L_t, (b) L_o, and (c) L_b.

and is assessed in units of buoyancy periods by comparing $N\overline{T'^2}$ to χ. *Dillon*'s [1982] analysis of data from the ocean's seasonal thermocline and wind-driven surface layer as well as the top few meters of a lake indicated τ_T to be almost always less than N^{-1} and always less than $2\pi N^{-1}$. It was argued that diffusive smoothing limited the ages of the energy-containing scales of the turbulence to something less than a buoyancy period.

Similarly, we can assess the decay time of the TKE due solely to viscous dissipation as

$$\tau_q = \frac{q^2}{\epsilon}. \tag{7}$$

Here we estimate the TKE, $q^2 = u_i u_i/2 \approx 3w^2/2$. This equality holds for isotropic turbulence and is a lower bound in the case of buoyancy-affected low Rey-

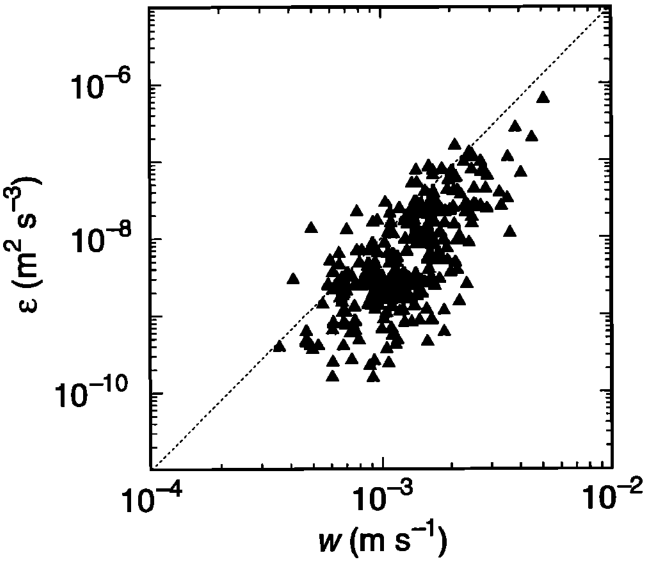

Figure 5. Rms vertical velocity w versus turbulent kinetic energy dissipation rate ϵ.

nolds number turbulence [*Gargett,* 1988]. However, all of these data are characterized by $Re_w \gg 1$, and we assume isotropy holds. In cases where buoyancy acts to preferentially attenuate w, this estimate of q^2 will result in an underestimate of τ_q. We compare Nq^2 to ϵ and estimate τ_q in units of buoyancy periods.

An evaluation of τ_q, τ_T is provided in Figure 10. The results are $0.67N^{-1} < \tau_T < 0.76N^{-1}$ (95% bootstrap confidence limts on the mean), with a mean value of $0.71N^{-1}$, and $1.9N^{-1} < \tau_q < 2.3N^{-1}$, with a mean value of $2.1N^{-1}$. Both mean values are considerably smaller than $2\pi N^{-1}$, in general agreement with *Dillon* [1982] and with *Crawford* [1986]. They are also significantly different from each other. The ratio of the mean values of the timescales is $\simeq 3$. The geometric mean value of the sample ratios of the two timescales is 2.87 (95% confidence interval 2.63, 3.14).

These estimates of decay timescales are based on the intermittent statistics of the turbulent field and are indirect. A direct measure would require observation of the temporal evolution of a turbulent patch following the complete removal of TKE sources. An approximation to this condition appears to be met following rainfall at the sea surface. *Smyth et al.* [1996] observed the rapid attenuation of turbulent dissipation rates beneath a stable, fresh layer of water, which served to isolate the preexisting mixed layer from surface forcing. They found the e-folding scale for the decay of ϵ below the squall layer to be $(0.3\text{–}1.0)2\pi N^{-1}$. This was considered an overestimate as TKE sources were not completely absent. It compares favorably with the indirect estimate made here of $(0.3\text{–}0.4)2\pi N^{-1}$.

4. Discussion

Despite scatter in individual data samples (as in Figures 3 and 4), there is now a history of consistent (and apparently repeatable) sets of observations showing $L_t = 1.1\text{–}1.2L_o$ [*Dillon,* 1982; *Crawford,* 1986; *Peters et al.,* 1995]. It seems plausible that a consistent relationship exists between L_b and L_t, L_o as well. Consequently, each of these scales is roughly representative of ℓ, although the choice of observationally derived length scale to represent ℓ imposes a systematic bias on its value. Consequently, parameterizations based on ℓ (such as the inviscid estimate of ϵ or the mixing length estimate of K_h) will have different constants of proportionality, depending on which length scale is used as a surrogate for ℓ.

Because the estimate L_b is based on the velocity scale, its use leads to a convenient reduction in the forms (1) and (5), where the velocity scale appears independently. Since it appears to provide as good an estimate of ℓ as any of the other length scales evaluated, there is no compromise in proceeding to use L_b in place of ℓ in (1) and (5). As a final note on the length scale comparisons, it seems that there is less scatter in dynamic length scale (L_b, L_o) comparisons and kinematic length scale comparisons (L_t, L_e) than there is between kinematic and dynamic length scales.

While the inviscid form for ϵ may be approximately correct, many values for the constant $C_\epsilon = \epsilon(\ell/u^3)$ have been published. These values, of course, depend

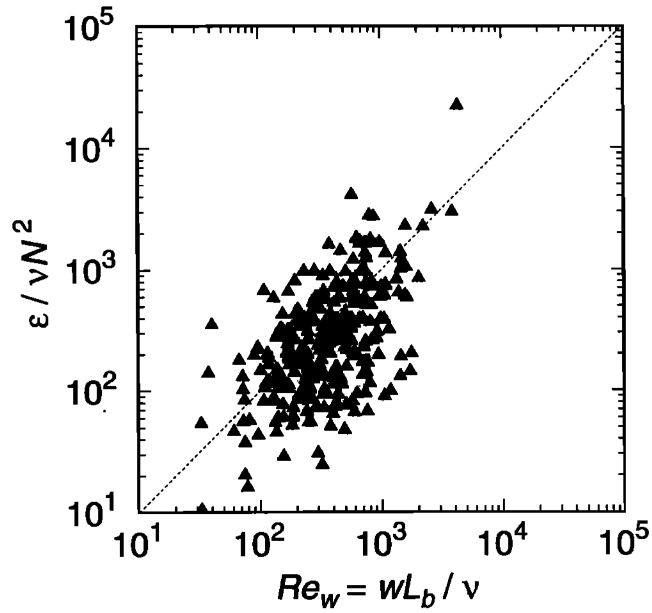

Figure 6. Vertical Reynolds number, $Re_w = w\ell/\nu$ (where ℓ has been replaced by L_b) versus $\epsilon/\nu N^2$. The parameter $\epsilon/\nu N^2$ is referred to as a buoyancy Reynolds number or turbulence activity.

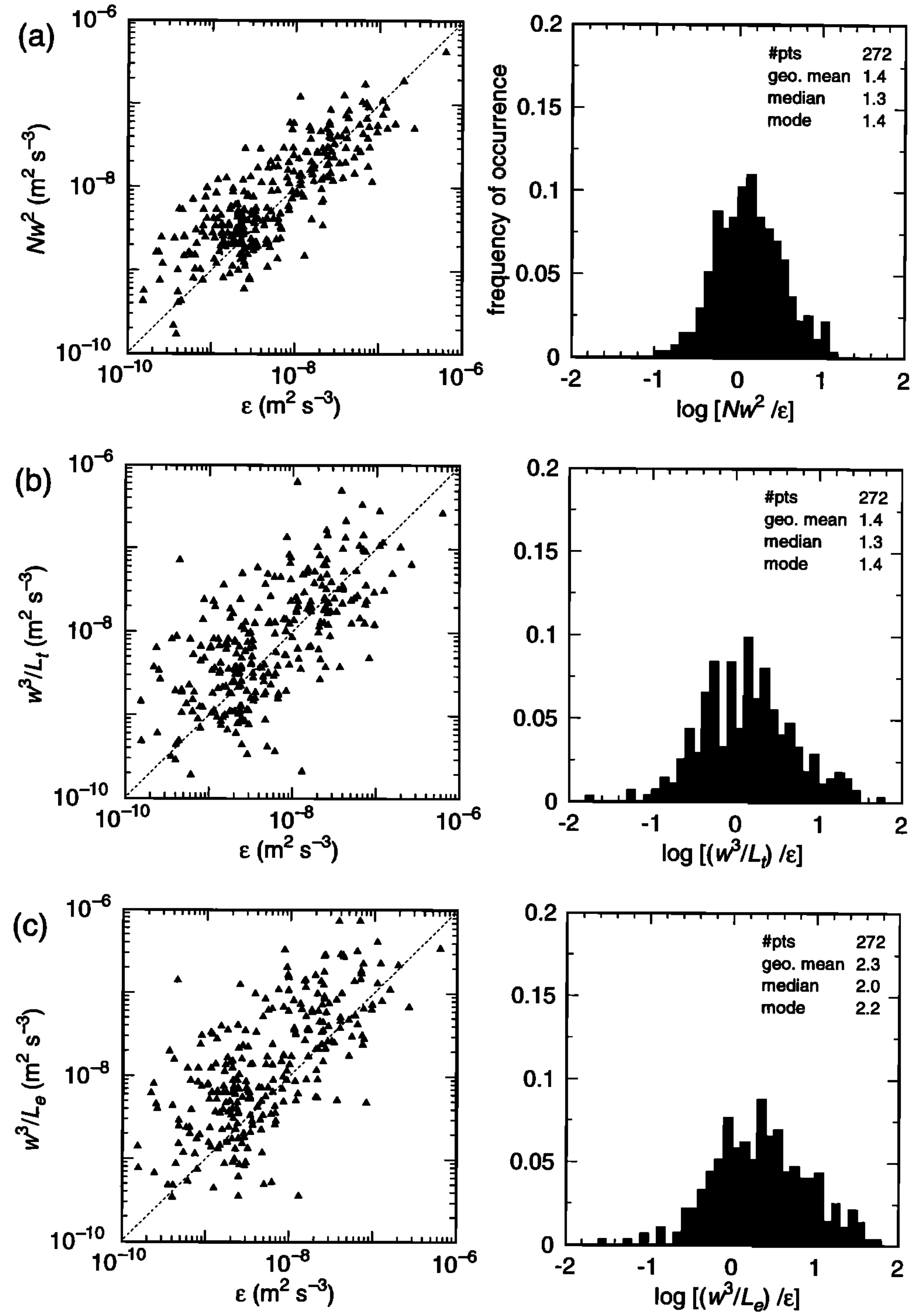

Figure 7. Comparison of the dissipation scale estimate ϵ and the inviscid or energy-containing scale estimates w^3/ℓ, where (a) $\ell = L_b = w/N$ and ℓ is replaced by (b) L_t and (c) L_e.

critically on the choice of velocity and length scales, which in turn are governed by the observational parameters available. This makes comparison difficult. Recent estimates of C_ϵ include relatively low values of 0.04 determined by *Brainerd and Gregg* [1993] from a model fit to turbulence in a restratifying mixed layer. However, *Smyth et al.* [1996] have provided a self-consistent scenario to indicate how this indirect estimate of C_ϵ may be severely underestimated due to a fundamental imbalance in the assumed TKE budget equation. Further estimates range through 0.125 from the stratified tank measurements of *Stillinger et al.* [1983] and *Itsweire et al.* [1986], which were reanalysed by *Ivey and Imberger* [1991]. *Hunt et al.* [1985] quote a value of C_ϵ = 0.4 – 0.6 for turbulent boundary layers, whether stable, neutral, or convective, and *Weinstock* [1981]

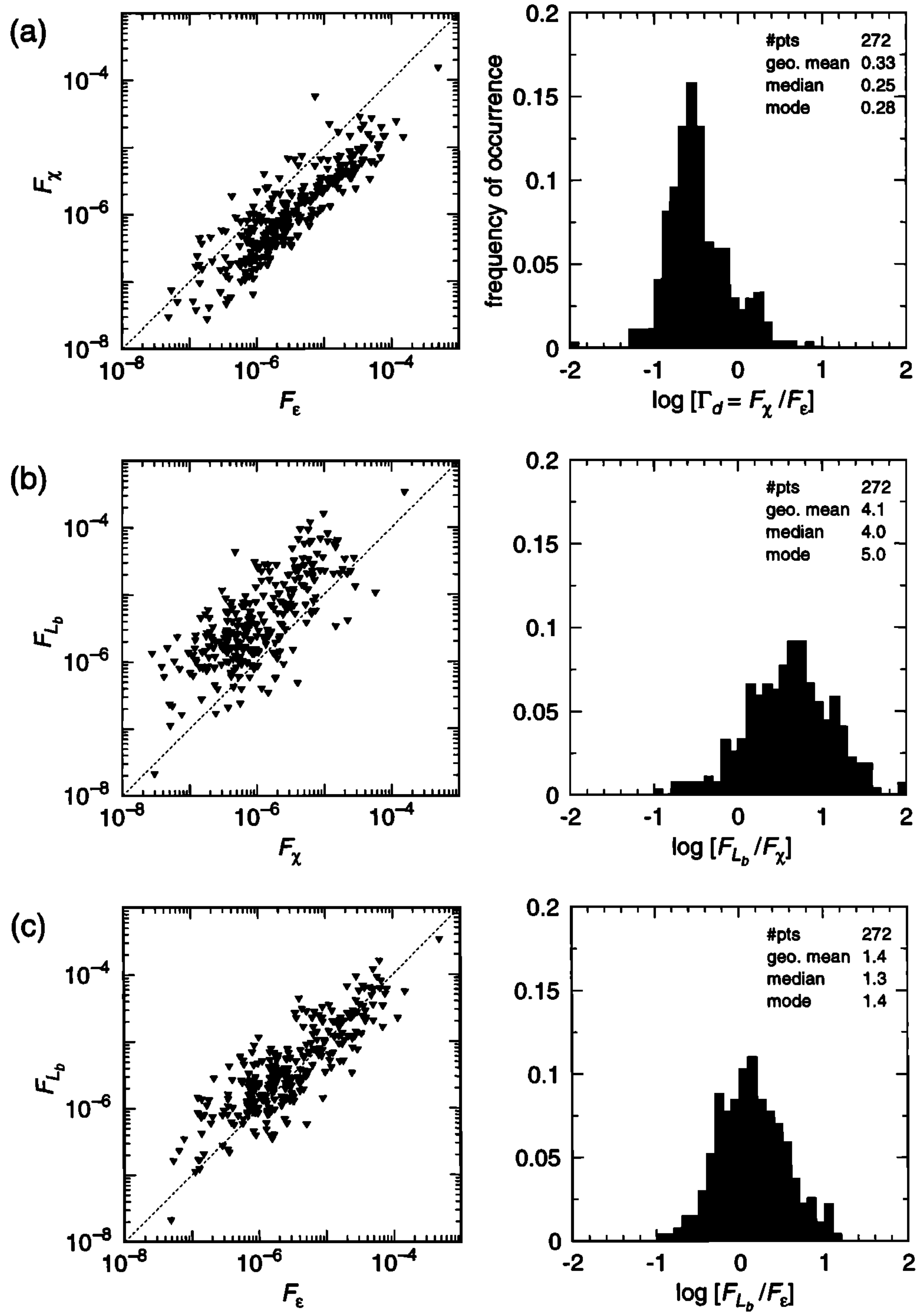

Figure 8. Comparison of heat flux estimates (a) F_χ versus F_ϵ, (b) F_{L_b} versus F_χ, and (c) F_{L_b} versus F_ϵ. The top right value N^2DC_x/ϵ is equivalent to Γ_d.

cites a value of 0.5 from theoretical considerations and 0.4 from statosphere data. Since these latter two studies use the rms vertical velocity for their velocity scale, their estimate is probably most similar to that determined in this study. However, Hunt et al. use an integral length scale for which there is no direct relative here or from any of the other studies. Higher values of 2-4 are reported by *Peters et al.* [1995]. *Wamser and Muller* [1977], *Kaimal and Haugen* [1967], and *Kaimal* [1973] estimated $C_\epsilon \sim 3$–5, away from boundaries.

Estimates of C_ϵ from these data, based on w and observed length scales, range from 0.4 to 1.2. Using $\ell = L_b$, $C_\epsilon = 0.7$ (Figure 7a). C_ϵ may be 0.7 or 0.6, depending on whether L_t or L_o is used. If L_e represents the appropriate length scale, $C_\epsilon = 0.4$. However, as explained by *Itsweire et al.* [1986], L_e is likely an un-

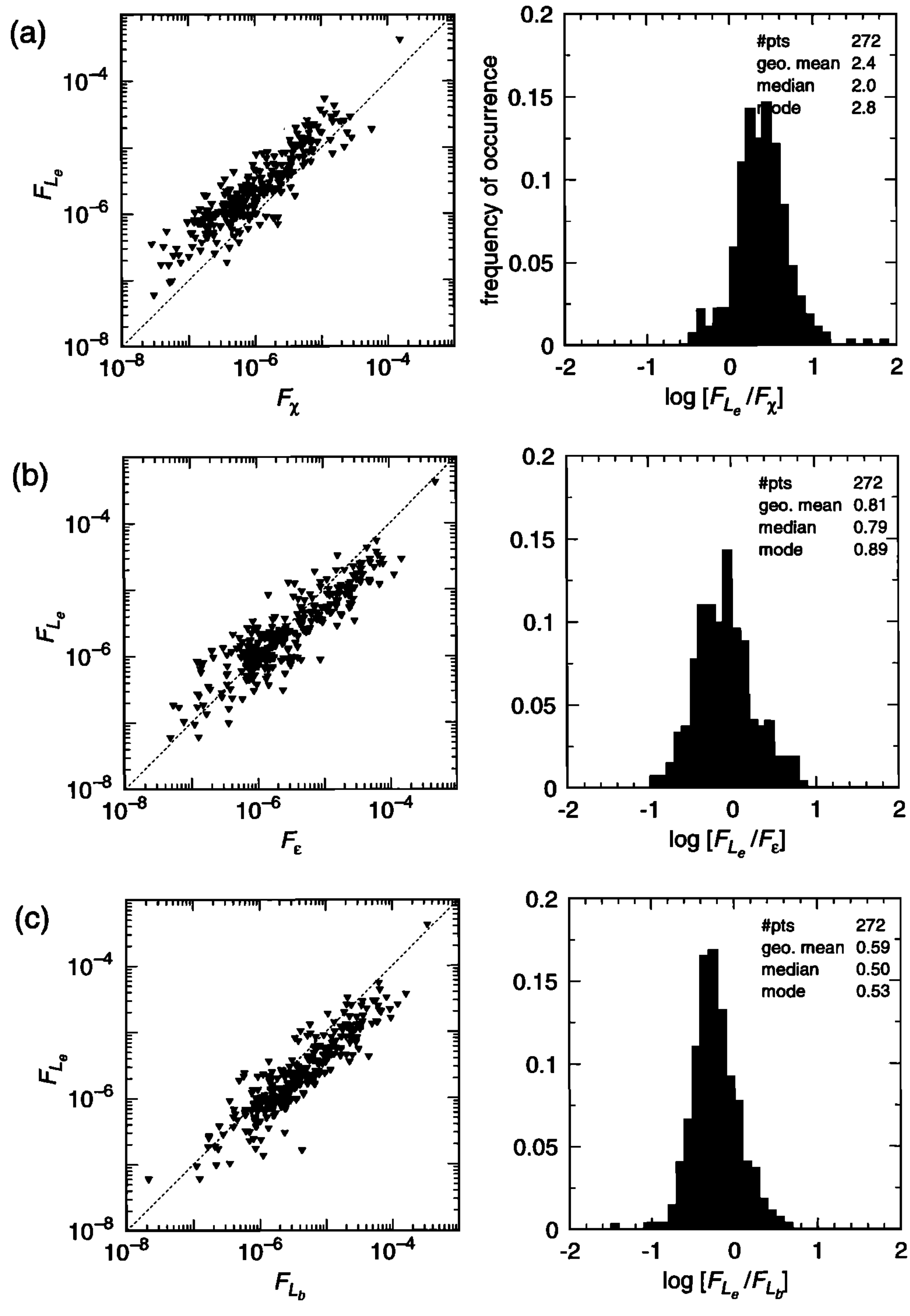

Figure 9. Comparison of the heat flux estimate F_{L_e} with (a) F_χ, (b) F_ϵ, and (c) F_{L_b}.

derestimate of the scale of the energy-containing eddies. *Stillinger et al.*'s [1983] choice is $2L_e$, giving $C_\epsilon = 0.8$, while *Gargett et al.*'s [1984] choice of $2\sqrt{2}L_e$ gives $C_\epsilon =$ 1.2, as does the choice of $1.67L_t$ used by *Peters et al.* [1995]. *Peters et al.* [1995] estimated C_ϵ to be 2.3–4.2, depending on the relative magnitudes of vertical to horizontal velocities. If, in the present study, the vertical velocity is attenuated by the stratification relative to the horizontal components, the estimates of C_ϵ made here will be upper bounds. However, there are no indications of such attenuation; Figure 7a indicates the same relative relationship between ϵ and Nw^2 even at very low values of ϵ, and as noted, $Re_w \gg 1$ for all of the data, and w is in good agreement with u_o in Figure 3c.

The coefficient C_ℓ in (5) is approximately 0.24 (95% confidence limits 0.21, 0.27), when L_b is substituted for ℓ. This is in close agreement to the value of 0.2 obtained

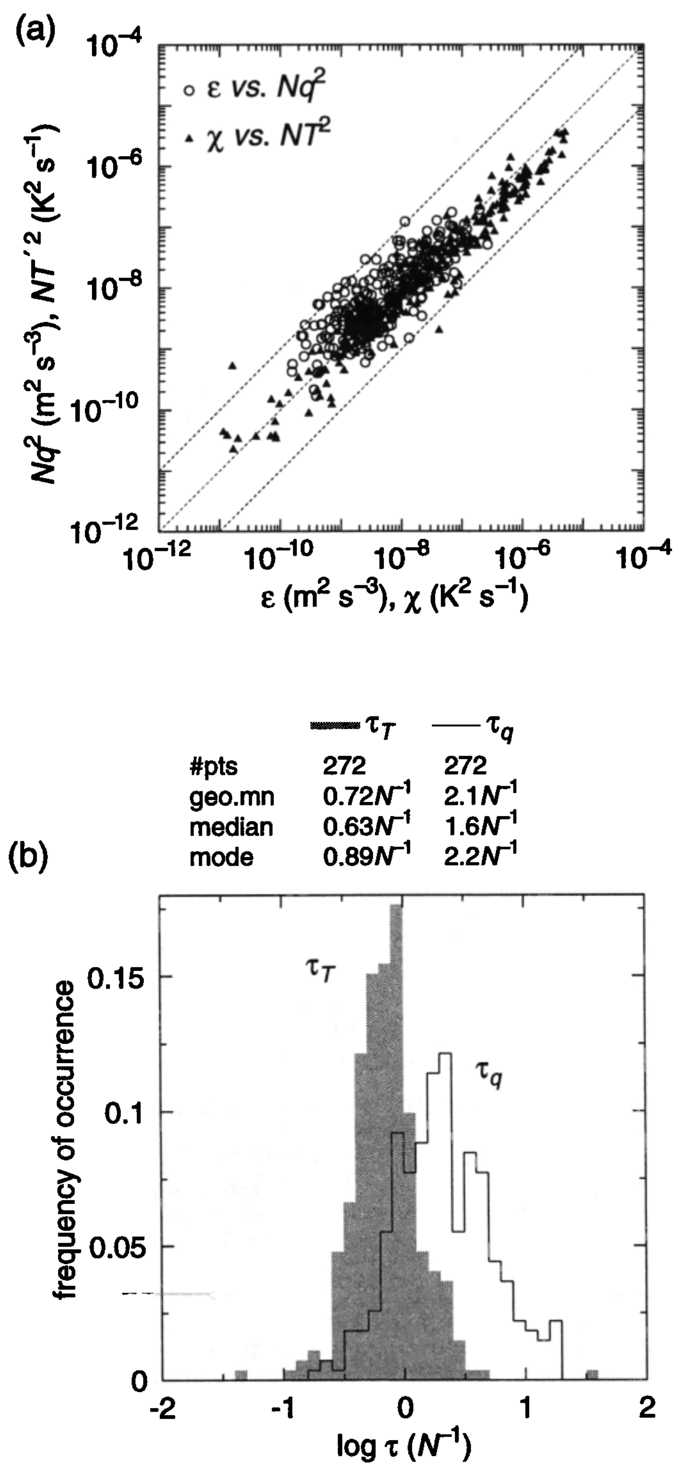

Figure 10. (a) Temperature variance dissipation rate χ plotted versus the product of the buoyancy frequency N and the turbulent temperature variance $\overline{T'^2}$ (triangles); turbulent kinetic energy dissipation rate ϵ plotted versus the product of N and the turbulent kinetic energy, $q^2 \sim 3w^2/2$ (circles). The dashed lines represent $Nq^2 = \epsilon$ or $N\overline{T'^2} = \chi$ and $Nq^2 = 0.1\epsilon$ or $N\overline{T'^2} = 0.1\chi$. (b) Histograms of the two timescales derived from equations (6) and (7), and the data shown in Figure 10a, in units of N^{-1}. Measures of central tendency indicate $\tau_T = \overline{T'^2}/\chi \sim 0.67N^{-1} - 0.71N^{-1}$ or $\approx$ $0.1(2\pi N^{-1})$, $\tau_q = q^2/\epsilon \sim 1.9N^{-1} - 2.3N^{-1}$ $\approx$ $(0.3 - 0.4)(2\pi N^{-1})$.

by *Hunt et al.* [1985] in the atmospheric boundary layer, also using w and L_b for velocity and length scales.

Why is $\tau_q > \tau_T$? It is possible that the cumulative uncertainties in determining τ_q and τ_T are sufficiently large that the two timescales are not significantly different; but this would require a systematic bias of a factor of 3 in the estimate of the ratio τ_q/τ_T, and we note that deviations from isotropy due to buoyancy effects will only cause τ_q to be underestimated, thereby increasing the difference between τ_q and τ_T. Let us suppose, then, that the observation $\tau_q > \tau_T$ is significant and consider what that means for the efficiency of the mixing process.

The dissipation flux estimates (2), (3) can be rewritten in terms of energy-containing scales using the observed values of τ_q and τ_T. Replacing ϵ by $Nq^2/2.1$ in (2), we obtain

$$F_\epsilon = \frac{q^2 T_z}{2.1N}, \tag{8}$$

and similarly replacing χ by $N\overline{T'^2}/0.7$ in (3),

$$F_\chi = \frac{0.5N\overline{T'^2}}{0.7T_z}. \tag{9}$$

Using these two forms, as in (4), gives the following expression for Γ_d,

$$\Gamma_d = \frac{\lambda N^2 \overline{T'^2}}{2T_z^2 q^2}, \tag{10}$$

where

$$\lambda = \frac{\tau_q}{\tau_T}. \tag{11}$$

From (10) and (11), we infer that $\Gamma_d \rightarrow 0$ for $\tau_q \ll \tau_T$. Conversely, Γ_d increases as τ_q increases relative to τ_T. This can be interpreted as follows. If the velocity fluctuations decay too rapidly (such that $\tau_q \ll \tau_T$), there exists insufficient time for significant irreversible mixing to occur by molecular conduction across concentration gradients. Consequently, very little of the kinetic energy available is converted to potential energy, i.e., $\Gamma_d \rightarrow 0$. Mixing will be more complete or more efficient if the turbulent motion persists past the time required to diffuse away the scalar gradients. By continued stretching of fluid parcels and coincident enhancement of concentration gradients at the smallest scales, a greater portion of their heat may be diffused into the ambient fluid. Of course, λ cannot increase without bound as Γ_d has practical limits [*Gargett and Moum,* 1995].

The scaling (10) for Γ_d suggests that λ is a fundamental parameter. If the other terms in (10) maintain their proportionality, then Γ_d can take on the observed value only if $\lambda \simeq 3$. Significantly different values of λ would result in significantly different values of Γ_d. The proportionality of the terms in (10) needs to be evaluated over a range of flow regimes. As (10) can be written

$$\Gamma_d = \frac{\lambda}{1.5}\left(\frac{L_e}{L_b}\right)^2, \qquad (12)$$

the ratio of timescales λ is important only so long as there exists a significant correspondence between these two length scales (as in Figure 4c).

5. Conclusions

The comparison of L_b to other estimates of ℓ is consistent with the interpretation of w, as measured from a pitot tube on a vertical microstructure profiler, as the energy-containing velocity scale of the turbulence in the upper part of the main thermocline. In particular, $L_b \simeq L_o$ implies $w \simeq u_o$, the buoyancy-modified velocity scale. The favorable comparison of L_b with the other energy-containing length scales derived from the observations gives us some confidence in using it in new formulations for dissipation and heat flux.

These new forms for turbulent dissipation and heat flux are as follows: (1) $\epsilon = C_\epsilon(u^3/\ell) \approx 0.7Nw^2$, 95% confidence range of C_ϵ is 0.67 – 0.79, and (2) $F_\ell = C_\ell u\ell T_z \approx 0.24(w^2/N)T_z$, 95% confidence range of C_ℓ is 0.21 – 0.27.

Estimates of each of these forms require a measure of the TKE, represented here by $3w^2/2$, and the background density and temperature profiles. These forms need to be evaluated in a broader range of flows using a variety of measurement techniques. Potentially, these may lead to more routine oceanic estimates of dissipation and heat flux.

These observations indicate that the timescales for both the viscous decay of turbulent motions and the diffusive smoothing of scalar fluctuations are smaller than $2\pi N^{-1}$. They also suggest that the turbulent motions last longer than the scalar fluctuations, a factor which serves to enhance the mixing efficiency of the turbulence.

We can probably claim a first-order understanding of the dynamics and kinematics of internal gravity waves in the ocean (at least at frequencies greater than inertial and significantly smaller than N) and of the dynamics of stratified turbulence at scales smaller than those containing most of the energy. However, we have only a muddied concept of the physics behind the behavior of the intermediate range of scales between the high vertical wavenumber gravity waves and the energy-containing scales of the turbulence. Improvements in our understanding of the turbulence generation and decay processes will only be achieved by pushing our observational and modeling capabilities toward that range of scales.

Acknowledgments. I am grateful to Bill Smyth and Chaojiao Sun for comments and especially to Doug Caldwell, who provided a critical assessment of an early version of this paper. This work was funded by the Office of Naval Research (grant N00014-89-J-3211).

References

Brainerd, K. E., and M. C. Gregg, Diurnal restratification and turbulence in the ocean surface mixed layer, 2, Modeling, *J. Geophys. Res.*, *98*, 22,657–22,664, 1993.

Crawford, W. R., A comparison of length scale and decay times of turbulence in stably stratified fluids, *J. Phys. Oceanogr.*, *16*, 1847–1854, 1986.

Dillon, T. M., Vertical overturns: A comparison of Thorpe and Ozmidov scales, *J. Geophys. Res.*, *87*, 541–549, 1982.

Ellison, T. H., Turbulent transport of heat and momentum from an infinite rough plane, *J. Fluid Mech.*, *2*, 456–466, 1957.

Fleury, M., and R. G. Lueck, Direct heat flux esimates using a towed body, *J. Phys. Oceanogr.*, *24*, 801–818, 1994.

Frisch, U., and S. A. Orszag, Turbulence: Challenges for theory and experiment, *Phys. Today*, *43(1)*, 24–32, 1990.

Gargett, A. E., The scaling of turbulence in the presence of stable stratification, *J. Geophys. Res.*, *93*, 5021–5036, 1988.

Gargett, A. E., Observing turbulence with a modified acoustic Doppler current profiler, *J. Atmos. Oceanic Technol.*, *11*, 1592–1610, 1994.

Gargett, A. E., and J.N. Moum, Mixing efficiencies in turbulent tidal fronts: Results from direct and indirect measurements of density flux, *J. Phys. Oceanogr.*, *25*, 2583–2608, 1995.

Gargett, A. E., T. R. Osborn, and P. Nasmyth, Local isotropy and the decay of turbulence in a stratified turbulence, *J. Fluid Mech.*, *144*, 231–280, 1984.

Gregg, M. C., Diapycnal mixing in the thermocline: A review, *J. Geophys. Res.*, *92*, 5249–5286, 1987.

Hebert, D., and J. N. Moum, Decay of a near-inertial wave, *J. Phys. Oceanogr.*, *24*, 2334–2351, 1994.

Hunt, J. C. R., J. C. Kaimal, and J. E. Gaynor, Some observations of turbulence structure in stable layers, *Q. J. R. Meteorol. Soc.*, *111*, 793–815, 1985.

Itsweire, E. C., Measurements of vertical overturns in a stably stratified turbulent flow, *Phys. Fluids*, *27*, 764–767, 1984.

Itsweire, E. C., K. N. Helland, and C. W. Van Atta, The evolution of grid-generated turbulence in a stably-stratified fluid, *J. Fluid Mech.*, *162*, 299–338, 1986.

Itsweire, E. C., J. R. Koseff, D. A. Briggs, and J. H. Ferziger, Turbulence in stratified shear flows: Implications for interpreting shear-induced mixing in the ocean, *J. Phys. Oceanogr.*, *23*, 1508–1522, 1993.

Ivey, G., and J. Imberger, On the nature of turbulence in a stratified fluid, *J. Phys. Oceanogr.*, *21*, 650–658, 1991.

Kaimal, J. C., Turbulence spectra, length scales and structure parameters in the stable surface layer, *Boundary Layer Meteorol.*, *4*, 289–309, 1973.

Kaimal, J. C., and D. A. Haugen, Characteristics of vertical velocity fluctuations observed on a 430 m tower, *Q. J. R. Meteorol. Soc.*, *93*, 305–317, 1967.

Lenschow, D. H. (Ed.), *Probing the Atmospheric Boundary Layer*, 269 pp., Am. Meteorol. Soc., Boston, Mass., 1986.

Lienhard, J. H., and C. W. Van Atta, The decay of turbulence in thermally-stratified flow, *J. Fluid Mech.*, *210*, 57–112, 1990.

Moum, J. N., The quest for K_ρ - Preliminary results from direct measurements of turbulent fluxes in the ocean, *J. Phys. Oceanogr.*, *20*, 1980–1984, 1990a.

Moum, J. N., Profiler measurements of vertical velocity microstructure in the ocean, *J. Atmos. Oceanic Technol.*, *7*, 323–333, 1990b.

Moum, J. N., Efficiency of mixing in the main thermocline, *J. Geophys. Res.*, in press, 1996.

Moum, J. N., M. C. Gregg, R.-C. Lien, and M.-E. Carr, Comparison of turbulent kinetic energy dissipation rate estimates from two ocean microstructure profilers, *J. Atmos. Oceanic Technol.*, *12*, 346–366, 1995.

Osborn, T. R., Estimates of the local rate of vertical diffusion from dissipation measurements, *J. Phys. Oceanogr.*, *10*, 83–89, 1980.

Osborn, T. R., and C. S. Cox, Oceanic fine structure, *Geophys. Fluid Dyn.*, *3*, 321–345, 1972.

Peters, H., M. C. Gregg, and J. M. Toole, On the parameterization of equatorial turbulence, *J. Geophys. Res.*, *93*, 1199–1218, 1988.

Peters, H., M. C. Gregg, and T. B. Sanford, Detail and scaling of turbulent overturns in the Pacific equatorial undercurrent, *J. Geophys. Res.*, *100*, 18,349–18,368, 1995.

Rohr, J., and C. W. Van Atta, Mixing efficiency in stably-stratified growing turbulence, *J. Geophys. Res.*, *92*, 5481–5488, 1987.

Smyth, W. D., P O. Zavialov, and J. N. Moum, Decay of turbulence in the upper ocean following sudden isolation from surface forcing, *J. Phys. Oceanogr.*, in press, 1996.

Stillinger, D. C., K. N. Helland, and C. W. Van Atta, Experiments on the transition of homogeneous turbulence to internal waves in a stratified fluid, *J. Fluid Mech.*, *131*, 91–122, 1983.

Taylor, G. I., Statistical theory of turbulence, *Proc. R. Soc. London A*, *151*, 421–454, 1935.

Tennekes, H., and J. L. Lumley, *A First Course in Turbulence*, 300 pp., MIT Press, Cambridge, Mass., 1972.

Thorpe, S. A., Turbulence and mixing in a Scottish loch, *Philos. Trans. R. Soc. London A*, *286*, 125–181, 1977.

Wamser, C., and H. Muller, On the spectral scale of wind fluctuations within and above the surface layer, *Q. J. R. Meteorol. Soc.*, *103*, 721–730, 1977.

Weinstock, J., Energy dissipation rates of turbulence in the stable free stratosphere, *J. Atmos. Sci.*, *38*, 880–883, 1981.

Yamazaki, H., and T. R. Osborn, Direct estimation of heat flux in the seasonal thermocline, *J. Phys. Oceanogr.*, *23*, 503–516, 1993.

J. N. Moum, College of Oceanic and Atmospheric Sciences, Oregon State University, 104 Ocean Admin Building, Corvallis, OR 97331-5503. (e-mail: moum@oce.orst.edu)

(Received September 25, 1995; revised January 11, 1996; accepted January 17, 1996.)